Synthesis and Characterization of Conjugated Polymers Containing First Row Transition Metal Complexes

Shengwen Yuan,[†] R. Jaramillo,[‡] T. F. Rosenbaum,[‡] and Luping Yu*,[†]

Department of Chemistry and The James Franck Institute, 5735 South Ellis Avenue, The University of Chicago, Chicago, Illinois 60637, and Department of Physics and The James Franck Institute, 929 E 57th Street, The University of Chicago, Chicago, Illinois 60637

Received June 27, 2006; Revised Manuscript Received September 27, 2006

ABSTRACT: A series of novel conjugated polymers containing first row transition metal complexes have been synthesized and characterized. Metal complexes including Mn(II), Fe(II), Co(II), Ni(II), and Cu(II) were incorporated into the bipyridine coordination sites of the conjugated polymer backbone. Upon inclusion of the metal complexes the absorption bands of the polymers were red-shifted and metal-to-ligand charge transfer (MLCT) bands were observed. The magnetic properties of these polymers were studied and the results showed that they all had high paramagnetic susceptibility; where applicable they were all stable in the high-spin state. Their large free spins and stability makes them promising as magnetic materials.

Introduction

The introduction of transition metal complexes into conjugated polymers brings new dimensions to the physical properties of this interesting class of semiconducting materials. Significant research efforts have been devoted to the synthesis of these new versions of conjugated polymers.[1−5] A variety of transition metal complexes are available, which have been either linked to the backbone as isolated pendants,[2] or inserted into the polymer backbone through coordination or covalent bonds.[1,3] The resulting conjugated polymers exhibit new redox, magnetic, and electronic properties, such as photoconductivity and photorefractive effects.[1−5] A wide range of applications have been investigated, such as dynamic holographic materials, organic light emitting diodes, and solar cells. Among these polymers, those containing late transition metals such as ruthenium, osmium, platinum, and iridium, have been studied most extensively due to the high stability of the associated complexes. However, the first row transition metal complexes are equally interesting, not only due to their abundance but also because of the unique magnetic properties associated with their partially occupied d-orbitals.[6−13] Magnetic molecules display many phenomena of fundamental interest such as variable effective dimensionalities, quantum size effects, and novel exchange interactions.[9−11] The tremendous potential of molecular magnets for applications has spurred efforts to raise the ordering temperature to technologically useful levels.[12] Making these materials particularly attractive for technological applications are a suite of physical properties that differentiate them from traditional solid-state magnets: such properties include mechanical flexibility, solubility, biocompatibility, intrinsic nanometer length scales, and a number of photoactive effects.[13] Thus, the study of $3d^n$ metal complexes in conjugated polymers is motivated by chemical, physical, and materials science demands.

Because of limited access to proper monomers and the instability of first row transition metal complexes, conjugated polymers bearing such complexes are rarely reported. In this paper, we present our efforts in synthesizing poly(*p*-phenylenevinylene) (PPV) with 2,2′-bipyrindinyl (bpy), 1,1,1,5,5,5-hexafluoroacetylacetonate (hfac) metal complexes. It was found that several metal monomer complexes survived the Heck reaction conditions. The manganese (II), iron (II), and copper-(II) complexes exhibited side reactions during polymerization; however, it was also found that a post-coordination reaction of these three metal complexes could restore the corresponding polymer complexes. Magnetic measurements showed that all metal ions in both the monomer and polymer complexes were in their respective high-spin states.

Results and Discussion

Monomer Synthesis and Characterization. Ligand monomer **1** was prepared by methods reported previously[1a] with a slight modification. In the last coupling step we used potassium *tert*-butoxide and THF as solvent instead of NaH and DME to obtain a better yield (90%). Scheme 1 outlines the approach to the synthesis of the first row transition metal complex monomers.

The structures of the metal complex monomers were characterized by both spectral and analytical methods. Selective combustion analysis for Co complex **2c** was consistent with the expected structure. Results from the MALDI mass spectrum analysis of the monomer complexes all show a strong peak due to the ion fragments with the mass corresponding to the molecules less a diketonate ligand. This may result from the instability of the molecular ions of the complexes generated by the MALDI instrument: one diketonate ligand may be lost before reaching the ion counter. FT-IR spectra for all complexes show strong peaks around 1635 cm^{-1}, corresponding to the C═O stretching vibration, and another three strong peaks around 1140−1260 cm^{-1}, corresponding to the C−F stretching vibration in the diketonate ligands.[14] These results provide the structures of the monomers (Table 1). It should be noted that the central absorption peak of C−F around 1205 cm^{-1} overlaps with the stretching vibration absorption of C−O (aryl carbon) at 1211 cm^{-1}.

The UV−vis spectra of the ligand monomer **1** and metal complex monomers **2a**−**e** are presented in Figure 1. The λ_{max}

* Corresponding author. E-mail: lupingyu@midway.uchicago.edu.
[†] Department of Chemistry and The James Franck Institute, The University of Chicago.
[‡] Department of Physics and The James Franck Institute, The University of Chicago.

10.1021/ma061447g CCC: $33.50
Published on Web 11/16/2006

Scheme 1. Synthesis of Complex Monomers 2a−e

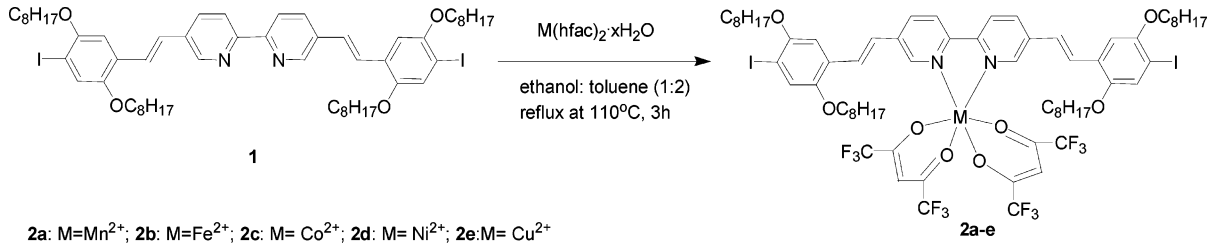

Scheme 2. Model Reaction of Cobalt Complex

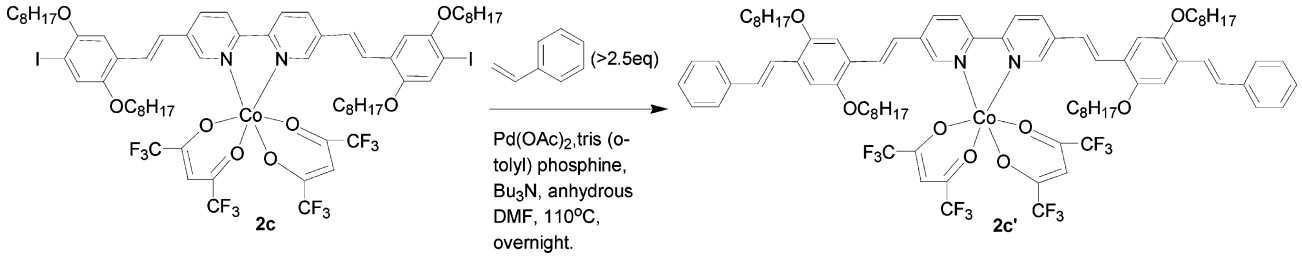

Table 1. Physical Properties of Ligand Monomer 1 and Complex Monomers 2a−e[a]

monomer	$\pi-\pi^*$ (nm)	ν(C−F) (cm^{-1})	ν(C═O) (cm^{-1})	$E_{1/2}$ (V)
1	397			0.953
2a	424	1147, 1205, 1256	1651	0.908
2b	428	1148, 1204, 1258	1628	0.918
2c	427	1149, 1206, 1257	1635	0.915
2d	428	1149, 1202, 1255	1640	0.906
2e	441	1145, 1202, 1257	1655	0.921

[a] Note: $E_{1/2}$ is the value vs the ferrocenium/ferrocene couple (Fc^+/Fc)

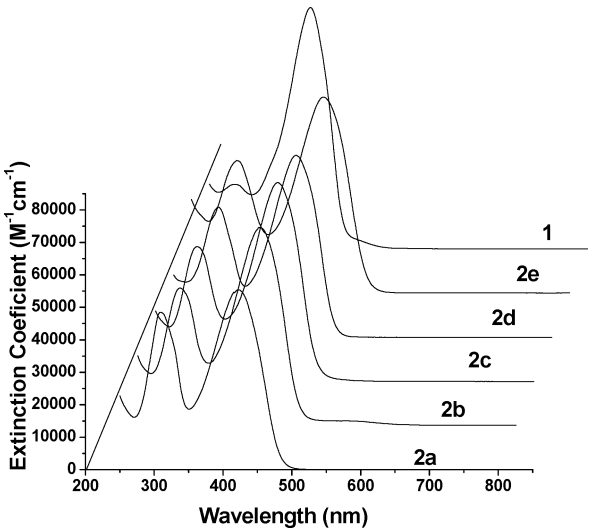

Figure 1. UV−vis spectra of ligand **1** and metal complex monomers **2a**−**e** in chloroform.

of the conjugated bipyridine ligand **1** (bpy) at 397 nm was red-shifted upon coordination with the metal diketonate (between 424 nm and 428 nm for Mn, Fe, Co, and Ni, and 441 nm for Cu), due to the effect of the metal ion's positive charge on the energy levels of the bpy ligand.[1d,15a] The red-shift of λ_{max} of Cu complex **2e** was about 15 nm more than that of the other four metal complexes **2a**−**d**, presumably due to stronger π back-bonding of the copper ion to the bpy ligand.[15b] The absorption resulting from the MLCT transition (around 450 nm) overlapped with that of the $\pi-\pi^*$ intraligand transition of bpy (around 423 nm).[1] Similar to its Ru complex counterpart, the MLCT band of the Fe complex **2b** extended further to about 620 nm;[1d] this extension was not observed in the other complexes. All complexes featured another absorption peak near 310 nm due to the $\pi-\pi^*$ intraligand transition of the diketonato.[14]

Model Reaction. Due to its mild reaction conditions, the Heck coupling reaction has been used in the synthesis of a wide range of functional conjugated polymers.[16] In this work, we used the Heck reaction for the polycondensation. First, a model reaction of the Co complex **2c** with an excess styrene was carried out to examine the stability of the metal complex under the Heck coupling condition (Scheme 2). The model product **2c′** was characterized by FT-IR, UV−vis, and elemental analysis. In its IR spectrum the strong absorption peak of C═O at 1636 cm^{-1} and those of C−F at 1147, 1206, and 1255 cm^{-1} were easily identified. Figure 2 shows the UV−vis spectra of the

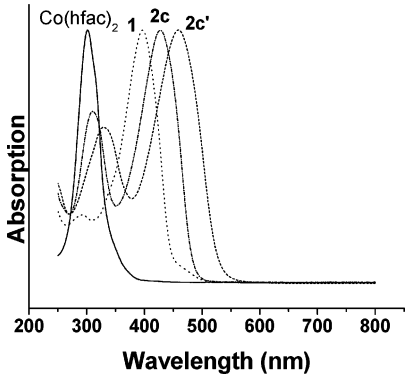

Figure 2. Comparison of the UV−vis spectra of ligand monomer and Co complexes.

Co(hfac)$_2$·xH$_2$O, Ligand **1**, Co complex monomer **2c**, and the Co model product **2c′**. We observed that λ_{max} of **2c′** was red-shifted relative to that of **2c** due to the elongation of the conjugation length of the bipyridine ligand. Combustion results were also consistent with the expected structure. These results proved the feasibility of further polymerization using the Heck coupling reaction.

Polymer Synthesis and Characterization. On the basis of the model reaction with the cobalt complex we carried out the Heck polycondensation of the diiodo-functionalized metal complex and 1,4-divinylbenzene. The polymerization reactions are shown in Scheme 3. The catalyst system consisted of 4% palladium acetate, 2.5 equiv of tributylamine, and 0.2 equiv of tris(*o*-tolyl)phosphine. The reaction mixtures in DMF were

Scheme 3. Synthesis of Complex Polymers 3c and 3d

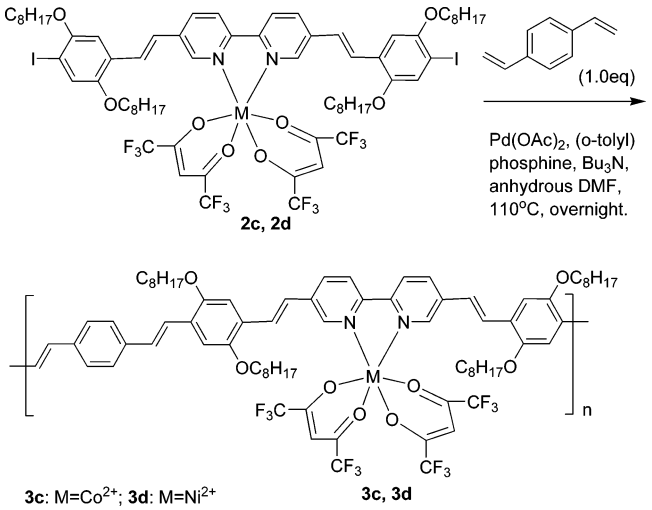

Scheme 4. Synthesis of Ligand Polymer 3 and Complex Polymer 4a, 4b, and 4e

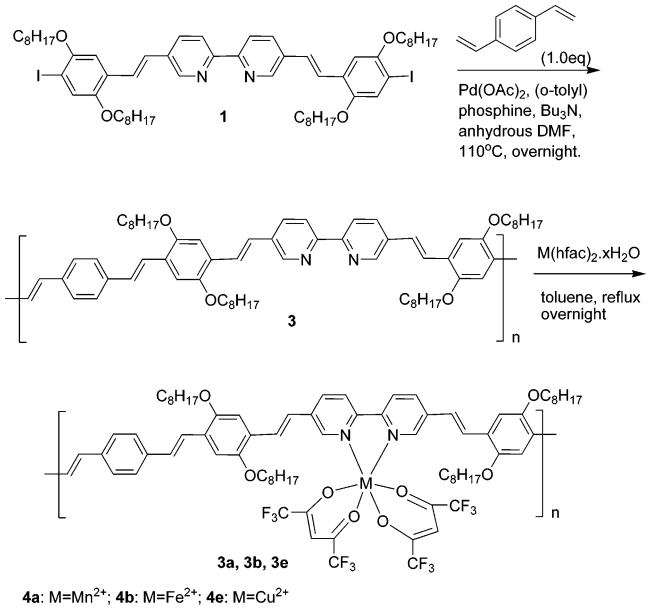

heated at 110 °C overnight. Crude products were precipitated into methanol and further purified by extraction in a Soxhlet extractor with methanol for 48 h. FT-IR spectra of the polymer thin films were used to monitor the presence of metal complexes. FTIR spectra were taken to confirm the presence of the metal complexes in the polymers. Ratios of absorption intensity of one of the C−F vibration bands around 1256 cm^{-1} over one of the C−H vibration bands around 2926 cm^{-1} were used to determine an approximate metal content in the polymers. If the metal complexes did not decompose after polymerization, the $I(\upsilon_{C-F})/I(\upsilon_{C-H})$ ratio in polymer should have an identical value with that in monomer. The ratios for the monomer and polymer complexes shown in the table below prove that the cobalt and nickel complexes survived the reaction conditions (the resulting polymers are named **3c** and **3d**, respectively), but some of the manganese, iron, and copper ions were lost during the polymerization (the resulting polymers are named **3a**, **3b**, and **3e**, respectively).

To obtain the polymers containing manganese, iron, and copper complexes (Scheme 4), we first synthesized a polymer **3** from the ligand **1**, and then carried out a subsequent coordination reaction of metal(II) bis(1,1,1,5,5,5-hexafluoro-2,4-pentandione) with polymer **3** in an equivalent ratio of the metal ions and the bipyridine coordination sites (mass of polymer **3** divided by the formula weight of its repeating unit gives the number of bipyridine sites). Three solvents, THF, chloroform, and toluene, were tested, and FT-IR spectra of the resulted polymers showed that toluene was the best solvent for this post-coordination reaction. The three polymers containing manganese, iron, and copper (**4a**, **4b**, and **4e**) were thus synthesized. For comparison, polymer **4c** and **4d** containing cobalt and nickel were also synthesized by post-coordination reaction. It should be noted that the coordination efficiency was less than 100 percent due to the decreased solubility of the resulting complex polymers in toluene, and therefore not all bipyridine sites were occupied by metal ions. Base on the metal content derived from the elemental analysis, we could see that iron and copper complexes have higher coordination efficiency than manganese complex. The physical properties of the polymers **3**, **4a**, **4b**, **3c**, **3d**, and **4e** are listed in Table 3.

Table 2. FT-IR Absorption Intensity Ratios of One of the C−F Vibration Bands around 1256 cm^{-1} over One of the C−H Vibration Bands around 2926 cm^{-1}

metal involved	Mn	Fe	Co	Ni	Cu
monomers $I(\upsilon_{C-F})/I(\upsilon_{C-H})$	**2a**	**2b**	**2c**	**2d**	**2e**
	1.8	1.8	1.72	1.85	1.55
polymers $I(\upsilon_{C-F})/I(\upsilon_{C-H})$	**3a**	**3b**	**3c**	**3d**	**3e**
	0.30	0.81	1.55	1.43	−

Table 3. Physical Properties of Polymers 3, 4a, 4b, 3c, 3d, and 4e[a]

polymer	$\pi-\pi^*$ (nm)	ν (C−F) (cm^{-1})	ν (C=O) (cm^{-1})	T_d (°C)	T_g (°C)	M_n	M_w	P_d
3	449			246	51	7200	19 100	2.65
4a	457	1145, 1201, 1256	1643	236	55	7400	15 900	2.15
4b	505	1144, 1201, 1256	1627	220	48	4300	5400	1.26
3c	467	1146, 1199, 1253	1637	256	58	4400	7700	1.75
3d	467	1148, 1202, 1256	1641	268	59			
4e	518	1144, 1201, 1257	1653	225	34	3200	3800	1.19

[a] T_d: Decomposition temperature (the onset temperature at the intersection of the first and second tangents); T_g: Glass transition temperature; M_n, M_w, and P_d were derived from GPC analysis based on polystyrene standards. FT-IR spectra were taken from a thin film of the polymers on NaCl plate.

Polymer **3** was readily soluble in many common organic solvents, such as tetrahydrafuran (THF), chloroform, methylene choloride, and toluene. The solubility of polymers **4a**, **4b**, **3c**, **3d**, and **4e** decreased significantly in the above solvents, but they could still be dissolved in THF or 1,1,2,2-tetrachloroethane to form a solution concentrated enough for the preparation of thin films.

The molecular weights of the polymers were characterized by GPC based on polystyrene standards (Table 2). Because of low solubility and low UV−vis absorption of the polymers **4a**, **4b**, **3c**, **3d**, and **4e**, some of their molecular weights were not conclusively determined. For example, polymer **4e** was prepared by coordinating copper(II) diketonate with polymer **3**, but its molecular weight was substantially lower than **3**. The molecular weight of polymer **3d** was not obtainable since its solubility in THF was particularly low, which might be an indication of a higher molecular weight. We should note that molecular weight of polymer **3** derived from the GPC is reliable because of its high solubility; the molecular weight of polymers **4a**, **4b**, **3c**, and **4e** are approximate values since their structure is much different from that of the standards.

The structure of all of the polymers was characterized by several spectroscopic techniques. Because of the existence of magnetic metal complexes, NMR spectra did not yield useful information. UV−vis spectra of all polymers are presented in

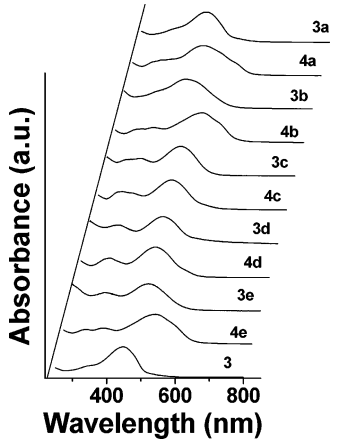

Figure 3. UV−vis spectra of ligand polymer and other metal-containing polymers in chloroform.

Figure 3. The UV−vis absorption peak of polymer **3** at 449 nm was red-shifted by about 52 nm compared with that of the ligand monomer **1** due to the longer conjugation length in the polymer. Polymers **4a**−**e**, **3c**, and **3d** showed strong absorption bands around 460−518 nm, which were red-shifted by 33−77 nm compared with the corresponding monomers. As in the monomers, metal complexes in the polymers lowered the energy levels of the polymer backbone by their positive charge effect on the bipyridine. An absorption shoulder around 560 nm for polymers **4a**, **4b**, and **4e** was clearly observed, corresponding to the MLCT transition. The $\pi-\pi^*$ transition of the diketonato ligand in polymers **4a**−**e**, **3c**, and **3d** appeared around 300 nm. UV−vis spectra of compound **3a** and **3b** were similar to that of polymer **3**, indicating partial elimination of the metal complexes, while most of the copper complexes may have survived in **3e**.

Similar to the monomers and the model compounds, the FT-IR spectra of polymers **4a**, **4b**, **3c**, **3d**, and **4e** exhibited C═O absorption bands around 1625−1655 cm^{-1} and C−F absorption bands around 1140−1260 cm^{-1}, indicating the incorporation of the metal bis(diketonate) into the polymer backbone (Table 2). These polymers exhibited CH_2 and CH_3 stretching vibration bands around 2850−2930 cm^{-1} and deformation bending vibration bands around 1460−1490 cm^{-1}. The absorption band at 965 cm^{-1} was from the out-of-plane bending vibration of the trans-substituted vinylene groups.

The thermal properties of these polymers were characterized by differential scanning calorimetry (DSC) and thermal gravimetric analysis (TGA); the results are summarized in Table 3. Polymers **4a**, **4b**, **3c**, **3d**, and **4e** have low glass transition temperatures T_g (around 55 °C), due to the existence of long alkyl side chains and the bulky metal complexes. The decomposition temperatures T_d of polymers **4a**, **4b** and **4e**, which were prepared by the post-coordination reaction, were found to be lower than that of polymer **3**. This is consistent with the results previously reported for ruthenium polymers[1] and further proved the presence of metal complexes.

Luminescence. As shown in Figure 4, all metal complex monomers **2a**−**e** had emission peaks around 535 nm, which were red-shifted by roughly 77 nm compared with the ligand monomer **1**; the emission peak of model compound **2c′** was red-shifted further to 582 nm. Polymers **4a**−**e**, **3c**, and **3d** exhibited emission peaks around 590 nm (Figure 5), which were red-shifted by roughly 75 nm compared with the ligand polymer **3**, while the emission spectra of polymers **3a** resembled that of **3**. This large red-shift upon incorporation of metal complexes is presumably due to the quenching of $\pi-\pi^*$ intraligand

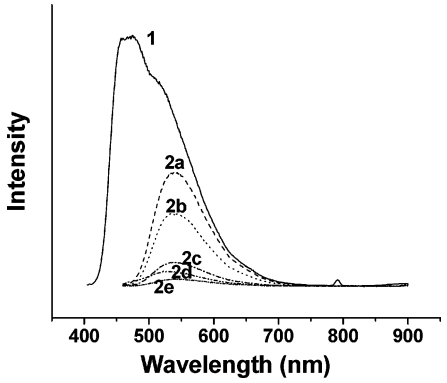

Figure 4. Emission spectra of all monomers in chloroform. Monomer **1** was excited at 395 nm and monomers **2a**−**e** were excited at 450 nm.

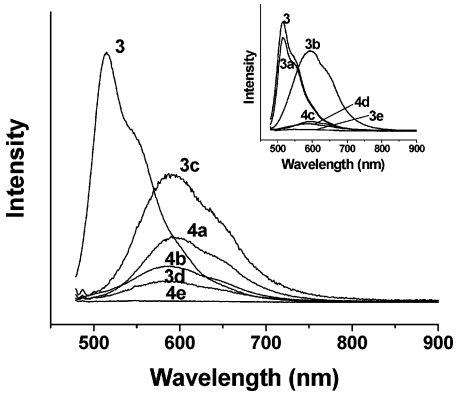

Figure 5. Emission spectra of polymers excited at 469 nm in chloroform (emission intensity was normalized by the concentration in g/mL). Inset is the emission spectra of polymers **3a**, **3b**, **3e**, and **4c**, **4d** for comparison. Emission intensity of polymer **3** and **3a** shown here has been scaled down 50 times to fit into the graph.

Table 4. Fluorescence Quantum Yield of Polymers 3 and 4a, 4b, 3c, 3d, and 4e in $CHCl_3$

	monomer		model	polymers					
	1	**2c** (Co)	**2c′**	**3**	**4a**	**4b**	**3c**	**3d**	**4e**
quantum yield	0.18	0.005	0.046	0.34	0.013	0.016	0.037	0.018	0.0012

transition by fast intramolecular energy transfer to the MLCT manifold, which is at a lower energy level.[17] Comparing the emission peaks of polymers **3**, **3c**, **3d**, and **4a**−**e** with those of their corresponding monomers **1** and **2a**−**e**, we saw a red shift of about 55 nm due to the longer conjugation length in the polymers. Quantum yields of monomers **1** and **2c**, model compound **2c′**, and polymers **3**, **4a**, **4b**, **3c**, **3d**, and **4e** in air-equilibrated chloroform were measured at room temperature (25 °C), using fluorescein in 0.1 M NaOH aqueous solution as a standard (Table 4). Upon incorporation of metal complexes the emission intensity decreased dramatically, presumably due to some nonradiative relaxation arising from spin−orbital coupling between the free spins of the metal ions and $\pi\pi^*$ orbitals of the bpy ligands. However, increasing the length of the conjugated ligand increased the quantum yield, as seen by comparing compounds **2c**, **2c′**, and **3c**, presumably because lowering the energy levels of $\pi\pi^*$ orbitals shifted their overlap with the dπ orbitals, thus somewhat suppressing nonradiative relaxation.

Cyclic Voltammetry. All monomer complexes have a reversible redox potential with $E_{1/2}$ around 0.91 V (vs Fc/Fc^+) arising from the diiodo-functionalized bipyridine ligand **1** (Table 1). The comonomer complex showed an irreversible oxidation wave at 0.754 V corresponding to oxidation of Co(II) to Co(III), and an irreversible reduction wave at −0.158 V corre-

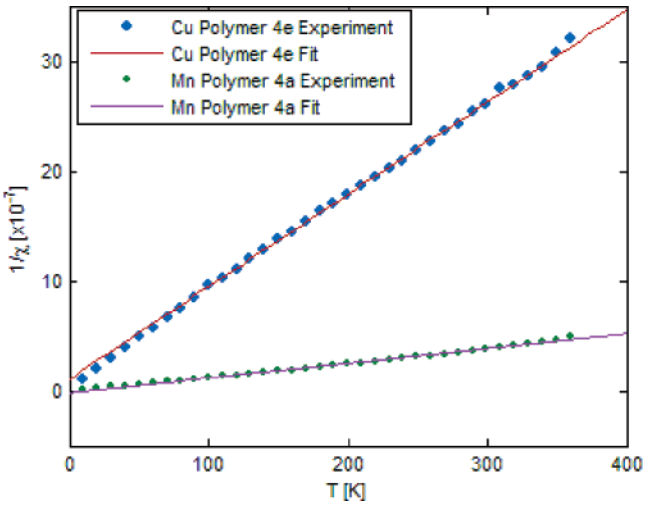

Figure 6. Inverse magnetic susceptibility vs temperature for polymers **4a** and **4e**. The measuring field is 1000 Oe. Linear fits obey eq 2; fit range is restricted to temperatures 100 K or greater. Symbol size approximates the extent of the vertical error bars. Susceptibility for sample **4a** has been normalized by the factor N_{4e}/N_{4a} for intercomparison, such that the slopes reflect the relative magnetic response of the two polymers, independent of sample size.

sponding to reduction of Co(II) to Co(I). The Fe monomer complex had a weak reversible reduction−oxidation couple with $E_{1/2} = 0.422$ V corresponding to Fe(II/III). The redox potentials for other metal ions could not be identified, presumably because they were too weak or overlapped with the ligand redox waves (or were outside of the studied potential range).[18] The $E_{1/2}$ of ligand **1** and polymer ligand **3** appeared at 0.953 and 0.860 V respectively, while $E_{1/2}$ of the Co model compound was 0.675 V. It seems that the elongation of conjugation and the incorporation of metal complexes both serve to lower the redox potential of the bipyridine ligand.

Paramagnetic Susceptibility. Due to the competition between electron pairing energy and the e_g-t_{2g} energy splitting, the d-electrons in d^4-d^7 systems may be distributed into either the high-spin or the low-spin state; for d^8 and d^9 systems these states overlap.[21] For 3d ions the spin−orbital interaction can be effectively ignored when compared with the crystal field interaction at ground state, and the orbital moment is quenched into the $L = 0$ state. This simplifies the calculation of the magnetic moment μ:

$$\frac{\mu}{\mu_B} = 2\sqrt{S(S+1)} \tag{1}$$

where μ_B is the Bohr magneton and S is the total electronic spin per ion. For small magnetic fields the susceptibility (in CGS units) is given by the Curie−Weiss law

$$\chi = \frac{N\mu^2}{3k_B(T-\Theta)} = C_{Curie}/(T-\Theta) \tag{2}$$

where k_B is Boltzmann's constant and N is the number of magnetic moments. This expression accounts for interactions between individual moments at the mean-field level.[21] A measurement of χ as a function of temperature allows one to solve for the magnetic moment μ, from which the spin state can be calculated using eq 1. In addition we can solve for the Weiss temperature Θ, which tells us the predominant sign of the coupling between individual magnetic moments (ferromagnetic or antiferromagnetic). As an illustration of the fitting procedure, Figure 6 shows the fits of eq 2 to the susceptibility data for polymer complexes **4a** and **4e**. As is customary, we fit only data above a minimum cutoff temperature, taken here as 100 K.

In Figure 7, we present the experimental results for μ/μ_B and Θ, along with the predictions for the high- and low-spin states. The metal content derived from elemental analysis has been taken into account in the determination of N for the polymer complexes. The experimental results for μ/μ_B indicated that all of the metal ions have the maximum possible number of unpaired electrons in their t_{2g} and e_g orbitals, a desirable condition for magnetic applications. It is worth noting that the

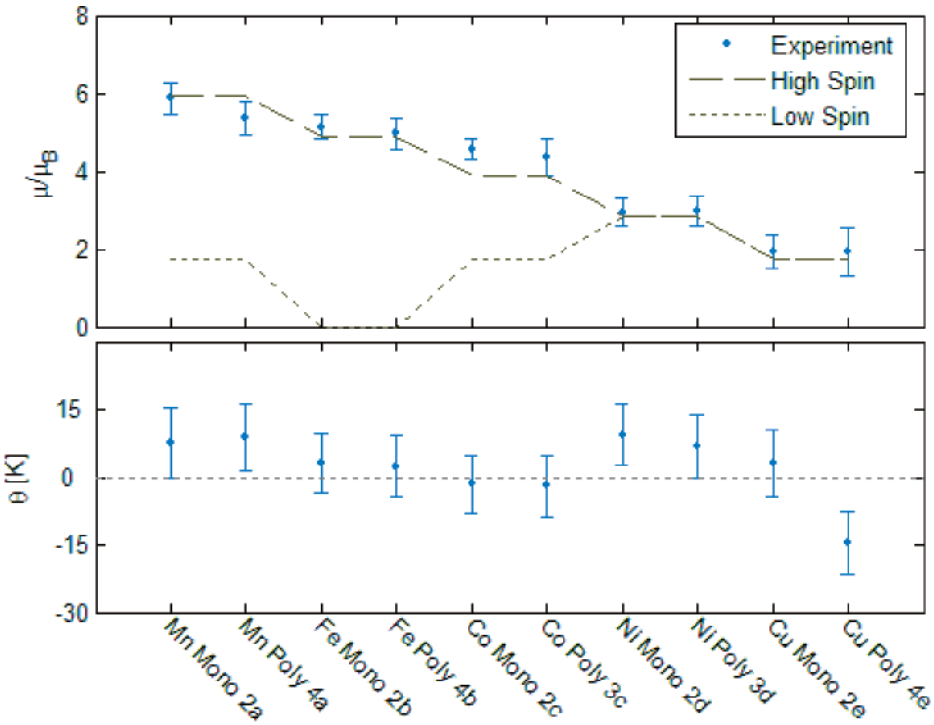

Figure 7. Magnetic moment and Weiss temperature, extracted from fits of eq 2 to susceptibility data.

d-electron spin state in the polymer complexes is the same as that in the corresponding monomers; the spins have not been quenched by the polymerization process.

We find evidence of small but finite couplings between magnetic moments for some of the complexes, as indicated by the Weiss temperatures Θ. In particular, we find that the Mn and Ni complexes exhibit weak ferromagnetic coupling, and that the Cu polymer is coupled antiferromagnetically. A finite Weiss temperature indicates the sign of the magnetic coupling and is not to be confused with an actual magnetic ordering temperature, which was not observed. Nonetheless, the observation of finite Weiss temperatures in some of our complexes is compelling given the large separation between magnetic ions along the polymer backbone (although we cannot at this point account for coincidental proximity effects, such as stacking). These results hold out the promise of engineering similar complexes with higher ordering temperatures. Given that our complexes are all stable in the high-spin state, they would make particularly strong molecular magnets. These materials are also possible candidates for physical studies on Faraday optical rotation and other magneto-otical effects.

Conclusion

A novel series of conjugated polymers bearing first row transition metal complexes were synthesized using Heck polycondensation or by metal complexation after polymerization. It was found that metal chelation introduced a large red-shift for conjugated polymeric ligand. In all of the polymers the metal ions stabilized in the high spin state. Although there was no significant spin−spin coupling through the conjugated ligands we do find finite Weiss temperatures for some of our complexes, pointing to the potential of long-range magnetic order at sufficiently low temperatures. The observed optical and magnetic properties in these materials are a good integration to the physical properties in semiconducting polymers. This conjugated polymer system has the flexibility of fine-tuning its properties by modifying its precursors' structure and metal content, thus providing an easy route to further investigations of the magnetic properties and potential applications of this new class of interesting materials.

Experimental Section

Materials. Tetrahydrofuran (THF) was distilled from Na^+/benzophenone ketyl. The *p*-divinylbenzene was separated from a mixture of *p*-divinylbenzene and *m*-divinylbenzene according to the published procedure.[19] Metals used in this work are manganese(II), iron(II), cobalt(II), nickel(II), and copper(II). Chemicals were purchased from the Aldrich Chemical Co. or Fisher Scientific Co. and used without further purification unless otherwise noted.

Equipment. The ^1H NMR spectra were collected on a Bruker 400 MHz FT NMR spectrometer. The FTIR spectra were recorded on a Thermo Nicolet Nexus 670 FTIR spectrometer. A Shimadzu UV-2401 PC spectrometer and a Shimadzu RF-5301 PC spectrofluorophotometer were used to record the absorption and emission spectra. The cyclic voltammetry was measured on a BASi CV-50W potentiostat Voltammetric analyzer interfaced to a personal computer. This experiment was carried out with a platinum wire working electrode, a platinum wire counter electrode, and a silver wire reference electrode. The supporting electrolyte used was 0.1 M tetrabutylammonium hexafluophosphate in dry dichloromethane for complex monomers. The half-wave potential $E_{1/2}$ was calculated using the equation $E_{1/2} = (E_{p,a} + E_{p,c})/2$, where $E_{p,a}$ and $E_{p,c}$ are the peak anodic and peak cathodic potentials, respectively. Thermal analyses were performed using a Shimadzu DSC-60 and a Shimadzu TGA-50 with a heating rate of 10 °C/min in a nitrogen atmosphere. Elemental analyses were performed by Atlantic Microlab, Inc. and Midwest Laboratories, Inc. Molecular weights were measured with a Water GPC system using polystyrene as the standards and THF as the eluent. The zero-frequency magnetic susceptibilities were measured using a Quantum Design MPMS SQUID magnetetometer. All samples were prepared for the measurements by packing dry power of the complexes into nonmagnetic capsules, which were then secured in the center of a (nonmagnetic) plastic drinking straw. Susceptibility was measured in the linear field regime (constant applied fields of 500, 1000, and 5000 Oe) at temperatures between 10 and 360 K, and the resulting data were fit to a Curie−Weiss law to solve for the spin state and the Weiss temperature.

Synthesis of Metal Complexes. Manganese(II), iron(II), nickel(II), and copper(II) diketonate hydrates were prepared following a general procedure in the literature;[20] water-soluble metal salts of $Mn(OAc)_2$, $FeCl_2$, $NiCl_2$, and $CuSO_4$ were used for the synthesis, respectively, and moderate yields of about 70% were obtained. Cobalt(II) hexafluoroacetylacetonate hydrate was purchased from Aldrich Chemical Co.

General Procedure for Metal Complex Monomers 2a—e. To a dry round-bottom flask equipped with a stir bar and a condenser was added ligand monomer **1** and 1 equiv of metal diketonate hydrate. The flask was evacuated and filled with nitrogen, and then absolute ethanol and toluene (1:2) were added. The resulting reaction mixture was refluxed at 110 °C for 3 h. After cooling, a large amount of hexane was added to the above mixture while stirring. The yellow or brown precipitate was collected by filtration, and further purified by precipitation from chloroform and hexane mixture. Anal. for compound **2c**. Calcd for $C_{68}H_{84}CoF_{12}I_2N_2O_8$: C, 51.11; H, 5.30. Found: C, 51.1, H, 5.32. MALDI MS for compound **2a**−**e**: base peaks corresponding to the complexes less one diketonate ligand were observed; the peak values were 1386, 1387, 1390, 1389, and 1394, respectively, consistent with the monomers' expected structure. Molecular ion peaks of the monomers were not easily identified due to the their instability as cations.

Synthesis of Model Compound 2c′. To a dry round-bottom flask equipped with a stir bar and a condenser was added complex monomer **2c** (0.08 g, 0.05 mmol)**,** styrene (0.015 mL, 0.125 mmol, 2.5 equiv), palladium acetate (4%mol), tri-*o*-tolylphosphene (20% mol), and tributylamine (3 equiv) and DMF anhydrous (3 mL). The resulting mixture was degassed and refluxed at 110 °C overnight under N_2 protection and then poured into methanol. The precipitate was collected, redissolved into chloroform and filtered through a pad of Celite. The filtrate was concentrated and reprecipitated into methanol. The resulting solid was collected and dried under vacuum. Anal. Calcd for $C_{84}H_{98}CoF_{12}N_2O_8$: C, 65.07; H, 6.37. Found: C, 65.17; H, 6.52. FTIR spectrum: Strong absorption was observed at 1637 cm^{-1} (C═O stretching vibration) and 1255, 1207, and 1148 cm^{-1} (C−F stretching vibration); these absorption peaks were also observed in the corresponding complex monomer **2c**.

General Procedure for Polymerization. To a dry round-bottom flask equipped with a stir bar and a condenser were added 1,4-divinylbenzene and 1 equiv of complex monomers **2a**−**e** or monomer ligand **1**, palladium acetate (4% mol), tri-*o*-tolylphosphene (20% mol), and tributylamine (2.5 equiv) and small amount of DMF (3−5 mL for every 0.04 g of 1,4-divinylbenzene). The resulting mixture was degassed and refluxed at 110 °C overnight under N_2 protection and then poured into methanol. The precipitate was collected by filtration and washed with methanol. The solid was further purified by extraction in a Soxhlet extractor with methanol for 2 days and then dried under vacuum.

General Procedure for Post-Coordination of Metal Diketonates with Polymer 3. To a dry round-bottom flask equipped with a stir bar and a condenser was added ligand polymer **3** and stoichiometric amounts of manganese(II), iron(II), or copper(II) diketonate, in accordance with the available bipyridine coordination sites (calculated by dividing the mass of polymer **3** by the formula weight of its repeating unit). The flask was evacuated and filled with nitrogen, and anhydrous toluene was added. The resulting reaction mixture was refluxed at 110 °C overnight. After cooling, large amounts of methanol were added to the above mixture while

stirring, and the resulting precipitation was collected, washed with methanol, and dried under vacuum.

Elemental Analyses. For the composition calculation, all polymers were assumed to have 8 repeating units base on the GPC analysis of polymer **3**. **Polymer 4a.** Anal. Calcd: C, 63.11; H, 6.25. Found: C, 70.81; H, 7.50. About 50% bpy sites were incorporated with manganese complexes. **Polymer 4b.** Anal. Calcd: C, 63.08; H, 6.24. Found: C, 65.50; H, 6.71. About 80% bpy sites were incorporated with iron complexes. **Polymer 3c.** Anal. Calcd: C, 62.94; H, 6.23; N, 1.88. Found: C, 66.28; H, 6.82; N, 2.10. About 75% bpy sites were incorporated with cobalt complexes. **Polymer 3d.** Anal. Calcd: C, 62.95; H, 6.23; N, 1.88. Found: C, 64.28; H, 6.50; N, 2.09. About 94% bpy sites were incorporated with nickel complexes. **Polymer 4e.** Anal. Calcd: C, 62.75; H, 6.21. Found: C, 63.71; H, 6.53. About 94% bpy sites were incorporated with copper complexes.

Acknowledgment. This work was supported by the NSF Materials Research Science and Engineering Center Grant DMR-0213745. R.J. gratefully acknowledges the support of a National Science Foundation Graduate Research Fellowship.

References and Notes

(1) (a) Peng, Z.; Yu, L. *J. Am. Chem. Soc.* **1996**, *118*, 3777. (b) Peng, Z.; Gharavi, A.; Yu, L. *J. Am. Chem. Soc.* **1997**, *119*, 4622. (c) Wang, Q.; Wang, L.; Yu, L. *J. Am. Chem. Soc.* **1998**, *120*, 12860. (d) Wang, Q.; Yu, L. *J. Am. Chem. Soc.* **2000**, *122*, 11806.

(2) Chen, X.; Liao, J.; Liang, Y.; Ahmed, M. O.; Tseng, H.; Chen, S. *J. Am. Chem. Soc.* **2003**, *125*, 636.

(3) Wilson, J. S.; Dhoot, A. S.; Seeley, A. J. A. B.; Khan, M. S.; Kohler, A.; Friend, R. H. *Nature (London)* **2001**, *413*, 828.

(4) Sandee, A. J.; Williams, C. K.; Evans, N. R.; Davies, J. E.; Boothby, C. E.; Kohler, A.; Friend, R. H.; Holmes, A. B. *J. Am. Chem. Soc.* **2004**, *126*, 7041.

(5) Maree, C. H. M.; Roosendaal, S. J.; Savenije, T. J.; Schropp, R. E. I.; Schaafsma, T. J.; Habraken, F. H. P. M. *J. Appl. Phys.* **1996**, *80*, 3381.

(6) (a) Cotton, F. A.; Holm, R. H. *J. Am. Chem. Soc.* **1960**, *82*, 2979. (b) Porter, L. C.; Dickman, M. H.; Doedens, R. J. *Inorg. Chem.* **1988**, *27*, 1549. (c) Sakane, A.; Kumada, H.; Karasawa, S.; Koga, N.; Iwamura, H. *Inorg. Chem.* **2000**, *39*, 2891. (d) Beghidja, C.; Rogez, G.; Kortus, J.; Wesolek, M.; Welter, R. *J. Am. Chem. Soc.* **2006**, *128*, 3140. (e) Miyasaka, H.; Clerac, R.; Wernsdorfer, W.; Lecren, L.; Bonhomme, C.; Sugiura, K.; Yamashita, M. *Angew. Chem., Int. Ed.* **2004**, *43*, 2801. (f) Girtu, M. A.; Wynn, C. M. *Phys. Rev. B* **2000**, *61*, 492. (g) Barra, A. L.; Caneschi, A.; Cornia, A.; Fabrizi de Biani, F.; Gatteschi, D.; Sangregorio, C.; Sessoli, R.; Sorace, L. *J. Am. Chem. Soc.* **1999**, *121*, 5302. (h) Preuss, E.; Richardson, J. F.; Bin-Salamon, S. *J. Am. Chem. Soc.* **2004**, *126*, 9942. (i) Saalfrank, R. W.; Trummer, S.; Reimann, U.; Chowdhry, M. M.; Hampel, F.; Waldmann, O. *Angew. Chem., Int. Ed.* **2000**, *39*, 3492. (j) Mitrikas, G.; Calle, C.; Schweiger, A. *Angew. Chem., Int. Ed.* **2005**, *44*, 3301.

(7) Galan-Mascaros, J. R.; Dunbar, K. R. *Angew. Chem., Int. Ed.* **2003**, *42*, 2289.

(8) Gatteschi, D.; Sessoli, R. *J. Magn. Magn. Mater.* **2004**, *272*−*276*, 1030.

(9) Gatteschi, D. *Philos. Trans. A* **1999**, *357*, 3079.

(10) Epstein, A. J. *MRS Bull.* **2000**, *25*, 33.

(11) Bludell, S. J.; Pratt, F. L. *J. Phys. Cond. Mater.* **2004**, *16*, R771.

(12) Verdaguer, M.; Bleuzen, A.; et al. *Philos. Trans. A* **1999**, *357*, 2959.

(13) Miller, J. S.; Epstein, A. J. *MRS Bull.* **2000**, *25*, 21.

(14) Moxon, N. T.; Moffett, J. H.; Gregson, A. K. *J. Inorg. Nucl. Chem.* **1981**, *43*, 2695.

(15) (a) Vance, F. W.; Hupp, J. T. *J. Am. Chem. Soc.* **1999**, *121*, 4047. (b) Katz, N. E.; Romero, I.; Llobet, A.; Parella, T.; Benet-Buchholz, J. *Eur. J. Inorg. Chem.* **2005**, 272.

(16) (a) Heitz, W.; Brugging, W.; Freund, L.; Gailberger, M.; Greiner, A.; Jung, H.; Kampschulte, U.; Niebner, N.; Osan, F. *Makromol. Chem.* **1991**, *192*, 967. (b) Suzuki, M.; Lim, J. C.; Saegusa, T. *Macromolecules* **1990**, *23*, 1574. (c) Weitzel, H. P.; Mullen, K. *Makromol. Chem.* **1990**, *191*, 2837. (d) Bao, Z.; Chen, Y.; Cai, R.; Yu, L. *Macromolecules* **1993**, *26*, 5281. (e) Bao, Z.; Chen, Y.; Yu, L. *Macromolecules* **1994**, *27*, 4629.

(17) Ley, K. D.; Schanze, K. S. *Coord. Chem. Rev.* **1998**, *171*, 187.

(18) Villamena, F. A.; Horak, V.; Crist, D. R. *Inorg. Chim. Acta* **2003**, *342*, 125.

(19) Strey, B. T. *J. Polym. Sci., Part A* **1965**, *3*, 265.

(20) Izumi, F.; Kurosawa, R.; Kawamoto, H.; Akaiwa, H. *Bull. Chem. Soc. Jpn.* **1975**, *48*, 3188.

(21) Blundel, S. *Magnetism in Condensed Matter*; Oxford University Press: Oxford, U.K., 2001.

MA061447G